AFRL-AFOSR-VA-TR-2018-0337

A Rydberg Atom Blockade Based Single Photon Source

James Shaffer
UNIVERSITY OF OKLAHOMA

08/26/2018
Final Report

Air Force Research Laboratory
AF Office Of Scientific Research (AFOSR)/ RTB1
Arlington, Virginia 22203
Air Force Materiel Command

REPORT DOCUMENTATION PAGE

Form Approved
OMB No. 0704-0188

1. REPORT DATE *(DD-MM-YYYY)*	2. REPORT TYPE	3. DATES COVERED *(From - To)*
19-08-2018	Final - this is a resubmission of a lost report	6/1/2012 - 11/30/2015

4. TITLE AND SUBTITLE
A Rydberg Atom Blockade Based Single Photon Source

5a. CONTRACT NUMBER
FA9550-12-1-0282

5b. GRANT NUMBER

5c. PROGRAM ELEMENT NUMBER

6. AUTHOR(S)
James P. Shaffer

5d. PROJECT NUMBER

5e. TASK NUMBER

5f. WORK UNIT NUMBER

7. PERFORMING ORGANIZATION NAME(S) AND ADDRESS(ES)
The University of Oklahoma
Office of Research Services
201 David L. Boren Blvd.
Norman, OK 73019-5300

8. PERFORMING ORGANIZATION REPORT NUMBER
105251900

9. SPONSORING/MONITORING AGENCY NAME(S) AND ADDRESS(ES)
Tatjana Curcic
Program Manager, Atomic and Molecular Physics Physics and Electronics
Directorate Air Force Office of Scientific Research/RSE
875 North Randolph St.
Arlington, VA 22203

10. SPONSOR/MONITOR'S ACRONYM(S)
AFOSR

11. SPONSOR/MONITOR'S REPORT NUMBER(S)

12. DISTRIBUTION/AVAILABILITY STATEMENT
Approved for release/ distribution unlimited

13. SUPPLEMENTARY NOTES
This submission is a recovery of an older report that has apparently been lost. I have subsequently moved institutions and do not have access to all of my files.

14. ABSTRACT

15. SUBJECT TERMS
Rydberg atoms, quantum optics, quantum physics

16. SECURITY CLASSIFICATION OF:			17. LIMITATION OF ABSTRACT	18. NUMBER OF PAGES	19a. NAME OF RESPONSIBLE PERSON
a. REPORT	b. ABSTRACT	c. THIS PAGE			James Shaffer
U	U	U	UU		19b. TELEPHONE NUMBER *(Include area code)* 226 791 4709

Final Report: A Rydberg Atom Blockade Based Single Photon Source AFOSR - FA9550-12-1-0282

James P. Shaffer

ABSTRACT:

We report on research dealing with transporting ultracold atoms into a high finesse cavity and generating quantum light using Rydberg atom blockade with the atoms collectively coupled to the cavity. Atom surface interactions are important in this research because the highly polarizable Rydberg atoms are within, ~100 μm, of dielectric surfaces (the mirror surfaces). A novel phenomenon on quartz was discovered and investigated, where Rb adsorbates induce negative electron affinity of the quartz surface enabling free electrons to bind to it. The electrons bind to the surface until they effectively cancel the electric field due to the Rb adsorbates. The electric fields at the surface were probed using the atoms and read-out using Rydberg atom electromagnetically induced transparency (EIT). The electric field measurements were supported by detailed calculations of the surface electric fields and band structure calculations. The project addressed important design criterion on how close structures, such as lenses, mirrors and surfaces, can be placed to atomic ensembles for atomic quantum engineering applications, particularly those based on Rydberg atoms. A high finesse cavity apparatus was constructed where ultracold atoms are placed inside a high finesse optical cavity to investigate quantum light production using Rydberg atom blockade. Calculations support the possibility of using the system for this purpose. Our calculations focussed on investigating single collective excitations to produce an on-demand single photon source. Trapping and using a single atom in a high-finesse cavity for a single photon source has been achieved, but it is technically challenging to load single atoms into a trap and couple the cavity field to the atom because the atomic absorption cross-section is small. The absorption cross-section can be increased by using an atomic ensemble, because the light-matter coupling can be enhanced using a collective state. It is also, in principle, more manageable to load an ensemble of atoms into a cavity and rely on Rydberg atom blockade to prepare single, collective excitations. The preparation scheme developed uses a Rydberg state to imprint correlations between atomic dipoles on a sample of noninteracting atoms within a Rydberg blockade radius. Only a controllable number of excitations can occur in the cavity mode volume due to Rydberg atom blockade so only that number of photons can be emitted by the cavity. Seven papers were published in refereed journals describing this work. The work was presented in 22 different international conference venues, including 5 invited talks. In addition, the work was described in 10 different invited colloquia.

REPORT:

Atom Surface Interactions:

The project addressed important design criterion on how close structures, such as lenses, mirrors and surfaces, can be placed to atomic ensembles for atomic quantum engineering applications, particularly those based on Rydberg atoms. We carried out work to show that the effect of surface adsorbates can be controlled on dielectric surfaces so that these types of experiments are possible. Surface adsorbates generate electric fields that can be detrimental to schemes where atoms are placed close to macroscopic physical objects. Due to recent technological advances in fabrication and atom trapping, hybrid quantum systems (HQS) consisting of atoms and surfaces, as well as electrons and surfaces, are fast emerging as ideal platforms for a diverse range of studies in quantum control, quantum simulation and computing, strongly correlated systems and microscopic probes of surfaces. The issue of atom-surface interactions naturally occurs in many quantum technological applications due to the desire to reduce system size. In many cases the atom-surface interactions can be detrimental. In particular, reduction in the size of chip surfaces is important to achieve large platform scalability in ion trapping, but decoherence and noise emerge as serious challenges as feature sizes shrink. Overcoming the effects of noise is a fundamental step in realizing the full potential of HQSs. Combining ultracold Rydberg atoms with surfaces for HQS is attractive because Rydberg atoms can have significant electric dipole moments and strong interactions which can be manipulated with optical fields. Experimental progress has been hampered by uncertainties in characterizing the interactions of atoms with surfaces.

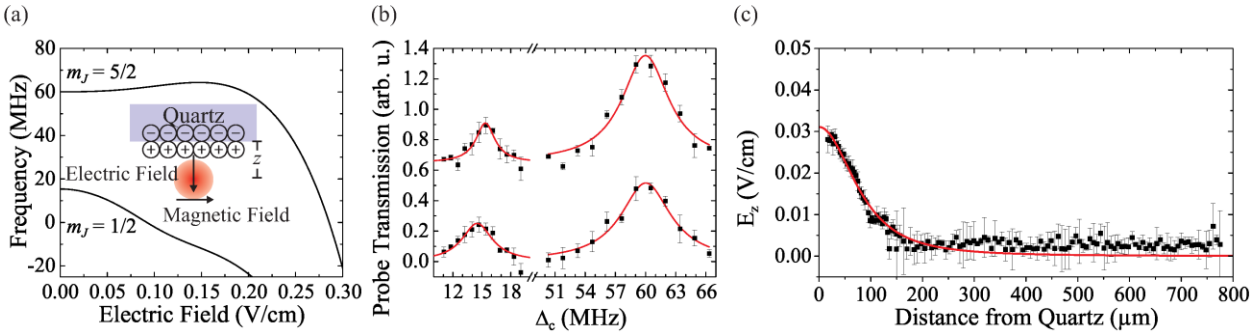

Figure 1: (a) Stark shift for $81D_{5/2}$, m_J =5/2 and 1=2 states in a 14.3 G magnetic field oriented perpendicular to the E-field. The inset shows the orientation of the electric and magnetic fields with respect to the quartz surface. (b) EIT spectra taken at two different positions z = 150 μm (upper) and z = 50 μm (lower) for $81D_{5/2}$ m_J = 1/2 (left) and m_J = 5/2 (right). The black points are pixel values of three averaged images, and the error bars are the standard deviation of the pixel values. The red lines are Lorentzian fits to the data. At z = 50 μm the m_J = 1/2 state is broadened and shifted corresponding to an E-field of 0.02Vcm^{-1}. (c) In the limit of large numbers of Rydberg atoms [Rb(81D)], the E-field is measured at distances of ~20–800 μm from the quartz surface at T_{sub} = 79 °C. Black points are taken from different pixels on a CCD camera. The error bars are the standard deviation of the measurement. The red line is a fit to Eq. (1), showing the inhomogeneity of the E-field. Our calculations indicate that the E- field at z<200 μm is caused by the large spacing between electrons that bind to the quartz surface.

To fully use Rydberg atom HQSs, a more complete understanding of surfaces is needed because the downside of coupling the 2 entities together is that they affect each other. For example, Rydberg atoms incident upon metal surfaces can be ionized and Rydberg atom energy levels can

be shifted by background electric fields (E-fields) caused by adsorbates. Rydberg states are sensitive to adsorbate E-fields because they are highly polarizable. Adsorbate E-fields have caused problems for a long list of experiments in other research areas such as Casimir-Polder measurements, and surface ion traps.

A convenient surface for applications in HQSs is quartz because of its extensive use in the semiconductor and optics industries – it is available in high quality forms with low surface roughness and high purity including as a single crystal. The (0001) surface has been the subject of recent theoretical interest, partially due to its stability and low surface energy. For these reasons, we chose to study a single crystal quartz (0001) surface.

In this grant period, we showed that adsorption of Rb atoms on a quartz (0001) surface, contrary to prevailing assumption, can reduce the E-field near the surface, Fig. 1. We demonstrated, by appealing to theoretical arguments and ab initio calculations, that the reduction in the E-field is caused by a transformation of the quartz-vacuum interface into a negative electron affinity (NEA) quartz surface via adsorption of Rb atoms. A NEA surface can bind electrons, similar to the image potential states on liquid helium (LHe). While the surface repulsion for electrons on LHe is provided by Pauli blocking, the repulsion on quartz occurs because the surface vacuum level dips below the conduction band minimum. We found that the binding of electrons to the surface substantially reduces the E-field above the surface.

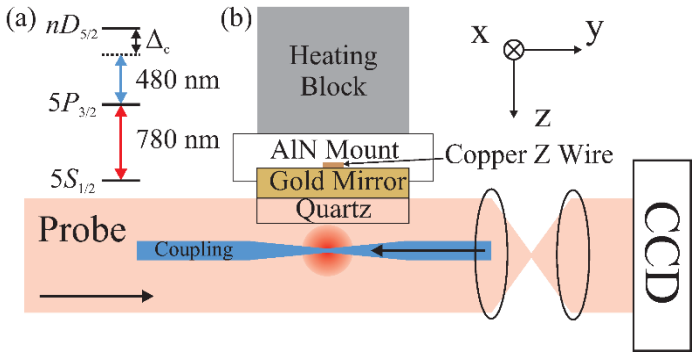

Figure 2: (a) Level scheme for Rydberg EIT used in our experiments. Δ_C is the coupling laser detuning. (b) A schematic of the experimental setup. Rb atoms are trapped in a mirror MOT, transferred into a magnetic trap, and transported to the surface. The probe and coupling beams for Rydberg EIT are overlapped and counter-propagate. The Rydberg EIT signal is observed by analyzing the absorption of the probe beam on a CCD camera. Heaters are placed outside of the vacuum to control the quartz temperature. The gold mirror is used to form the MOT. The heating block controls the temperature of the substrate. The Z wire generates the magnetic trap. The aluminum nitride (AlN) mount insulates the Z wire from the heating block.

In our setup, Fig. 2, a cloud of ultracold atoms is generated in a mirror magneto-optic trap (MOT) and used to load a magnetic z-trap formed with a z-shaped wire and an external bias magnetic field. The spatial resolution in the atom-surface separation that we have used is determined by the optical setup for absorption imaging and the signal to noise ratio of the EIT signal. We used a spatial resolution of $\sim 5\mu$m for the data presented in this report. We use a 150 mW 780 nm diode laser system for the probe laser and an amplified 960 nm frequency doubled diode laser system that produces > 200mW of 480nm light for the coupling laser. Both lasers are stabilized to an ultrastable Fabry-Perot cavity (Stable Laser) with offset locks that can be tuned. We achieved Rydberg atom EIT linewidths of less than 300 kHz. We showed that the traps work with both LaF_3 and quartz. Both materials are

birefringent, but we have no problems creating a MOT. Fig. 3 shows Rydberg atom EIT data taken close to a 500 μm thick z-cut quartz crystal at several different temperatures using several different Rydberg states. The data shown in Fig. 3 demonstrates that we can measure E-fields as close as 10 μm to the surface. We observed signals as close as 5 μm. The difficulty in obtaining a

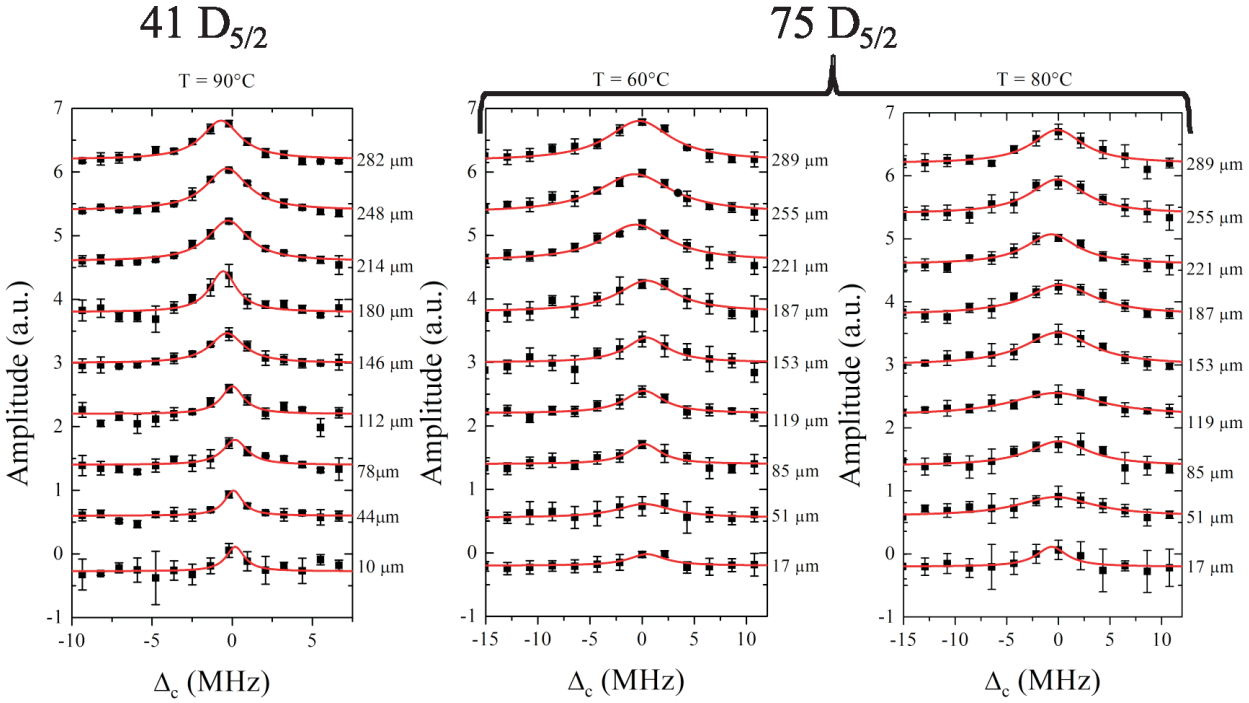

Figure 3: These plots show EIT signals taken for several Rydberg states at different atom-surface separations as a function of coupling laser frequency. Three different substrate temperatures are shown. The material was a 500μm thick piece of z-cut, (0001) surface normal, quartz. The surface roughness was < 5 Å. The data from these graphs can be used to determine that the electric field due to Rb sticking on the surface of the quartz is < 50mVcm^{-1} at ~ 20μm atom-surface separation by analyzing the Rydberg atom Stark shifts.

usable signal closer to the surface is that scattering of the coupling laser from the surface causes ions to form as part of the light induced atomic desorption (LIAD) process. The ions generate small inhomogeneous electric fields corresponding to ~ 10 mV cm^{-1}. The LIAD effects can be eliminated by careful alignment and shaping of the Gaussian coupling beam. The falloff of the intensity of a Gaussian beam makes it difficult to avoid LIAD induced electric fields and obtain usable EIT signals closer to the surface.

The E-fields are determined experimentally by measuring the frequency shift of a Rydberg state, and comparing it to a Stark shift calculation. Stark shifts of two magnetic states for $81D_{5/2}$ m_J =5/2 and m_J =1/2 are shown in Fig. 1(a). An example of the experimental traces at different z is shown in Fig. 1(b). These types of traces, also see Fig. 3, were used to obtain the E-fields. The Rydberg state energy is determined using Rb Rydberg atom EIT, Fig. 2(a).

A microscopic picture of E-field noise is obtained by considering thermal fluctuations of adsorbate dipole moments. An adsorbed atom develops a dipole moment as a result of the polarization of the

adatom in interaction with the surface. As the density of adsorbates increases, the E-field from neighboring dipoles reduces the dipole moment of each adatom. We estimated the dipole moment for a Rb adsorbate in the limit of small coverage to be d_0 =12 D. Adsorption of a large number of Rb atoms on the quartz surface then produces macroscopic E-fields. At distances far from the surface, the E-field can be modeled as two square sheets of charge, with edge length L, separated by a small distance. Near the center of the sheets, the E-field is largely perpendicular to the surface,

$$E_z = \frac{2\sqrt{2}\,\sigma\, d(\sigma) L^2}{\pi\epsilon_0\sqrt{L^2+2z^2}(L^2+4z^2)} \qquad (1)$$

where ϵ_0 is the permittivity of free space, σ is the adsorbate density, and d(σ) is the coverage dependent dipole moment. The temperature dependence of σ is

$$\frac{\sigma/\sigma_0}{1-\sigma/\sigma_0} = Ce^{\left(\frac{E_a}{KT_{sub}}\right)} \qquad (2)$$

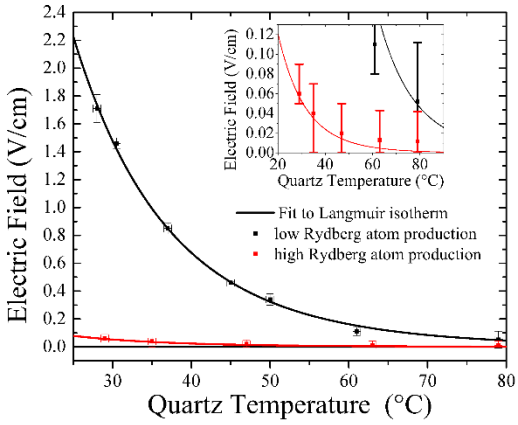

Figure 4: The measured E fields due to Rb adsorbates on the (0001) surface of quartz as a function temperature T_{sub} at a distance of 500 μm from the surface. The E fields are calculated by analyzing the frequency shifts of the EIT spectra. The black points are in the limit of low Rydberg atom production. The black line is a fit to the Langmuir isobar of Eq. (2), and yields a desorption activation energy of E_a = 0.66 ± 0.02 eV. The red data points were taken with high Rydberg atom production. The red line is explained in the text. The horizontal error bars are due to the uncertainty in the temperature T_{sub}. The vertical errors bars are the standard deviation of the experimental data. In the case of high- (low-) Rydberg atom production, the Rabi frequencies of the probe and coupling lasers are $\Omega_p = 2\pi \times 3.5$ MHz and $\Omega_c = 2\pi \times 4$ MHz. Approximately 200 electrons are produced during each experimental sequence, with a 10 Hz average rate. The horizontal error bars are due to the uncertainty in T_{sub} and are ±0.5 °C.

where σ_0 is the density of adsorbate sites, E_a is the desorption activation energy, k is the Boltzmann constant, and T_{sub} is the substrate temperature. Equations (1) and (2) relate E_z to σ at T_{sub}.

We measured the E-field as a function of T_{sub}. The results are shown in Fig. 4 at z = 500 μm. At 28 °C for small numbers of excited, probe Rydberg atoms (black line in Fig. 4), the E-field is 1.7 ± 0.1 V cm^{-1}. Using Eq. (1), for a slab of length L = 10 mm and $d_0 \sim 12$D, we estimate $\sigma = 4\times10^5$ atoms μm^{-2}, yielding an average Rb spacing of 1.5 nm, and an adatom coverage of 11%. Fitting all values of σ to Eq. (2) with a coverage dependent dipole moment yields E_a = 0.66 ± 0.02 eV. E_a is as expected given the activation energies measured for alkali atoms on other similar surfaces.

For the data shown in Fig. 4, it is clear that one way to minimize surface E-fields caused by Rb sticking to the surface is to heat the crystal. For the modest temperatures shown in Fig. 4 the E-fields are <50mVcm^{-1} at distances of around 10−20 μm. This is consistent with data we have obtained in thermal vapor

cells which was the first to investigate E-fields at surfaces using Rydberg atom EIT. We have also analyzed the uniformity of coverage of the substrate using the theoretical fits in Fig. 1(c) and 4. Our analysis yield large patch sizes, ~ 1-10 mm, indicating highly homogeneous electric fields. We showed that the surface E-field is constant as a function of atom-surface distance, as expected from a uniform, infinite sheet of dipoles, consistent with Rb binding with surface terminated oxygen atoms. The data we have presented shows that surface E-fields can be probed precisely using Rydberg atom EIT.

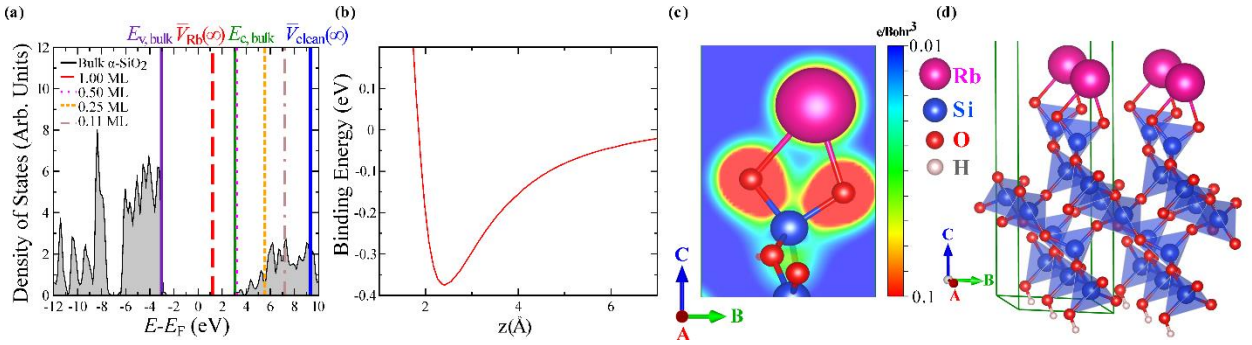

Figure 5: (a) Density of states of bulk α-quartz. The Fermi level EF is at E = 0. The valence band maximum $E_{v;bulk}$ and conduction band minimum $E_{c;bulk}$ of bulk α-quartz, and the vacuum levels of the SiO2(0001) surface without and with Rb adsorbates, respectively, $\bar{V}_{clean}(\infty)$ and $\bar{V}_{Rb}(\infty)$, are labeled. $\bar{V}_{Rb}(\infty)$ is shown as a function of coverage in fractions of a monolayer (ML). Increasing the amount of Rb coverage shifts the vacuum level down in energy. With one ML of Rb on the surface (red line), the vacuum energy dips below the bottom of the conduction band (green line), indicating the formation of a NEA surface. (b) Binding energy as a function of z for the Rb atom bound to an oxygen atom. (c) Electron density plot of Rb-O2. (d) Calculational cell for Rb surface calculations.

Increasing the Rydberg atom number in either trap dramatically reduces the E-field, Fig. 4 (red line), by increasing the flux of slow blackbody ionized electrons that can bind to the surface. The Rydberg atom number can be made larger by increasing the probe laser Rabi frequency. The temperature dependence of the reduced E-field is shown in Fig. 4 (red line). For typical data in Fig. 4 (red line), 300 atoms are ionized per experimental sequence. Rb(nS) and Rb(nD) states were investigated for $40 \leq n \leq 100$, yielding similar results.

The Rydberg atoms are predominately ionized due to blackbody radiation; direct blackbody ionization accounts for 99% of all electrons at high n. For Rb $81D_{5/2}$, the electrons have an average kinetic energy of 10 meV. For n ~ 40–100, the electrons average kinetic energy is 8–15 meV. If blackbody ionized electrons can bind to the surface, they can neutralize the E-field produced by the Rb adatoms. Electrons can bind to a conducting or dielectric surface through their image potential. These states are usually ultrashort lived, and rapidly collapse into the bulk. In LHe, however, the Pauli repulsion provides the necessary barrier of ~1 eV to prevent decay, leading to the formation of stable bound states on the surface. In LHe, the electrons can remain in these states for tens of hours at cryogenic temperatures. For adsorption on ordinary surfaces, if the vacuum energy dips below the bottom of the conduction band, a NEA surface is produced, repelling electrons from the surface. Amorphous quartz has a positive electron affinity of 0.9 eV. However,

the adsorption of Rb atoms can change the surface properties. The dipole layer created by the Rb adsorbates changes the electric potential at the vacuum-surface interface, Fig. 5(a). By calculating the electrostatic change in energy of an electron transported across the surface dipole layer, an estimate of the change in electron affinity $\Delta\chi$ can be made. Using d_0 = 12 D and $\sigma = 4.2 \times 10^5$ atoms μm^{-2} at T_{sub}=28 °C, the change in surface electron affinity is $\Delta\chi = -1.9$ eV. This approximation suggests that Rb at our densities can shift the vacuum level ~1 eV below the conduction band, inducing a NEA surface on quartz. The model shows a NEA up to $T_{sub} \sim 40$ °C. To investigate the adatom-surface on a microscopic level, we performed total-energy calculations for the quartz (0001) surface with various Rb coverages using spin-polarized density functional theory (DFT). On the surface of quartz, the Rb atom is bound to two oxygen atoms, Fig. 5(c). The lowest bound state for one monolayer (ML) has an energy of E_b=0.35 eV, Fig. 5(b). For the lower experimentally investigated coverages, our DFT calculations show an increase of E_b by ~1.4. The calculated E_b is comparable in magnitude with the measured E_a, and is consistent with the expectation $E_b \leq E_a$. We calculated the electronic density of states for bulk α-quartz and the shift of the vacuum energy with varying amounts of Rb coverage using DFT, Fig. 5(a). The Fermi level EF is set equal to zero, and lies in the middle of the band gap, between the top of the valance band $E_{v;bulk}$= 3.05 eV, and the bottom of the conduction band $E_{c;bulk}$ = 3.05 eV. As shown in Fig. 5(a), the vacuum level for the clean surface, $V_{clean}(\infty)$, has a positive electron affinity, consistent with experiment. However, adsorbing Rb on the surface shifts the vacuum level downward. A NEA is induced around 0.5 ML. The DFT and the straightforward electrostatic calculations both show that the vacuum level shifts by several electron volts with only a modest amount of Rb coverage. The remaining discrepancy may be resolved with further improvements in DFT. More knowledge of the experimental surface including the Rb adsorbate structure will also help to guide the calculations.

For high temperatures and a high Rydberg population the E-field is low. The measured E-field as a function of z at T_{sub} = 79 °C is shown in Fig. 1(c). For z>200 μm the E-field is negligible within error. At z<200 μm the E-field increases to ~30 mV cm^{-1}. Under these conditions, we estimate a surface electron density of ~10 electron mm^{-2}. We model the electrons as a uniformly charged square sheet of length L, which overlays the adsorbate layers at z = 0. The resulting E-field is a sum of the E-fields from the adsorbates and electrons, $E_{tot} = E_{ads} + E_{ele}$. After requiring E_{tot}=0 at z = 0, $E_{tot}(z)$ at z = 500 μm is plotted in Fig. 1(c). The near exact fit to the data is an indication that the reduction in the E-field is due to the formation of a NEA surface for Rb-SiO2. For z< 200 μm, approximating the electrons as a uniform sheet of charge breaks down since the electron spacing becomes larger than z. The spectral width of the EIT resonance for $81D_{5/2}$, m_J=1/2 increases from 2 MHz far from the surface to ~4 MHz at $z \leq 50$ μm, Fig. 1(b). We attribute this broadening to the inhomogeneity of E_{tot} near the surface. The data in Fig. 1(c) are fit to Eq. (1), and show that the residual E-field can be modeled as a dipole patch, with L ~ 200 μm, approximately equal to the estimated electron spacing of ~300 μm.

We can remove electrons from the surface using 400 nm light generated by a light emitting diode array. With the surface saturated with electrons [$E_{tot}(z = 0)= 0$], the light emitting diodes are pulsed on for a variable time while atoms are loaded into the MOT. The light intensity is small to avoid the light induced desorption of Rb. The MOT fluorescence is monitored to verify this condition. The photodesorption rate constant has an Arrhenius behavior, with an activation energy of 0.7 ± 0.07 eV. The activation energy is similar to E_a, suggesting the electron detachment mechanism is dependent on Rb coverage. The Rb coverage affects the energy levels most strongly. It is unknown if the electrons are detached from or tunnel into the surface. The electron photodetachment is the subject of future investigation.

Collective Excitations in a High Finesse Cavity:

We also investigated collectively preparing atoms using Rydberg atom dipole blockade in the new dipole trap loaded optical cavity apparatus. We showed theoretically that interesting collective atomic states can be prepared in an optical cavity using Rydberg atom dipole blockade as an integral tool. The preparation of these types of states can be important for developing single photon sources and other interesting light sources like superradiant lasers. Trapping and using a single atom in a high-finesse cavity for a single photon source has been achieved, but it is technically challenging to load single atoms into a trap and couple the cavity field to the atom because the atomic absorption cross-section is small. The absorption cross-section can be increased by using an atomic ensemble, because the light-matter coupling can be enhanced with a collective state. It is also, in principle, more manageable to load an ensemble of atoms into a cavity and rely on Rydberg atom blockade to prepare single excitations in the cavity. The preparation scheme is shown in Fig. 6. The scheme uses a Rydberg state to imprint correlations between atomic dipoles on a sample of noninteracting atoms within a Rydberg blockade radius. A single collective Rb $5P_{3/2}$ excitation can be created because the Rydberg atom interactions block the excitation of more than one Rydberg atom at a time. Creating collective excitations in a cavity enables the of study super atom excitation dynamics, since the photons created in the cavity mode are a signature of the initial atomic state that was prepared. During the course of our work, we have become interested in whether or not Rydberg atom blockade can be used to synthesize more elaborate quantum states and, if so, how can this best be accomplished?

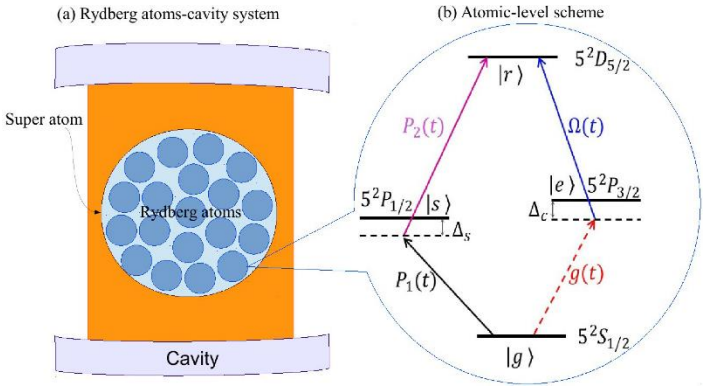

Figure 6: (a) Collectively prepared atoms coupled to a cavity within a Rydberg blockade radius. (b) Level scheme of a four-level atomic system driven by three laser pulses on transitions $|g\rangle \leftrightarrow |s\rangle$, $|s\rangle \leftrightarrow |r\rangle$ and $|r\rangle \leftrightarrow |e\rangle$ with Rabi frequencies $P_1(t)$, $P_2(t)$ and $\Omega(t)$ respectively. The transition $|g\rangle \leftrightarrow |e\rangle$ is coupled to the cavity with coupling strength $g(t)$. Γ_r is the decay rate of the Rydberg state, Γ_0 is the spontaneous decay rate of the $|e\rangle$ state and κ is the cavity decay rate.

We began initial studies of the system shown in Fig. 6 to excite variable numbers of collective excitations in a high finesse optical cavity to investigate synthesizing different types of collective quantum states.

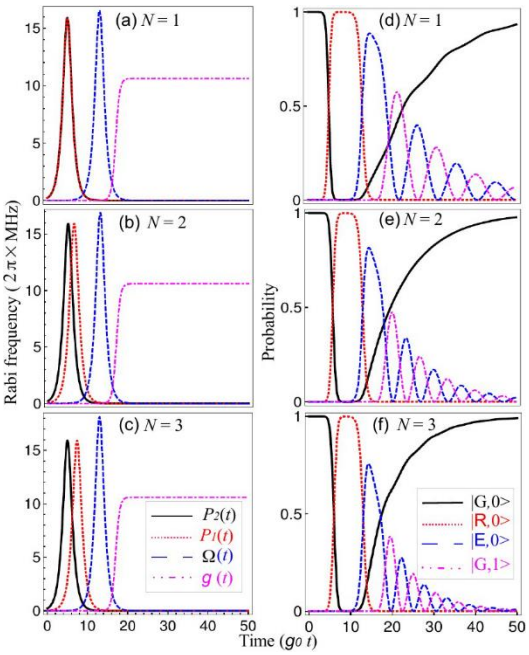

Figure 7: Rabi Oscillations: Figure (a-c) shows time variations of Rabi frequencies of the laser pulses applied in four-level system for N interacting atoms and Figure (d-f) are the corresponding probabilities. Parameters for the calculation are $\Gamma_r = 2\pi \times 4.4$ kHz, $\Gamma_e = 2\pi \times 5.2$ MHz, cavity detuning $\Delta_c = 0$, cavity decay rate $\kappa = 0.1 g_0$ and $\Delta_s = 64$ MHz.

We have theoretically showed that it is possible to observe Rabi oscillations in an ensemble of N atoms by creating a single collective excitation in the $5P_{3/2}$ state of Rb coupled to a cavity field mode by using Rydberg atom dipole blockade as shown in Fig. 6. The Rabi oscillations are enhanced by $\sqrt{N}$ times the cavity coupling strength, g_0, showing that a super atom has been created, Fig. 7. One side of the ladder system shown in Fig. 6 is used to collectively excite the atoms to the Rydberg level using a pair of π-pulses or a pair of counterintuitive STIRAP pulses with Rabi frequencies $P_{1,2}(t)$. By using a control laser pulse, $\Omega(t)$, a single photon can be generated in the cavity, Fig. 6-7. A full many-body calculation with all possible states was done for up to 3 atoms. Our calculations include the decay mechanisms that affect the interacting many-body system and show that the maximum photon efficiency for emission into the cavity with number of atoms depends on the spontaneous emission rate of the collective state which can be increased by the Purcell factor. This N interacting atoms-cavity system is well within the reach of experimental realization. The calculations show promise that the scheme is useful for single photon generation, building up complicated superposition states of the atomic ensemble by repeated applications of the excitation pulses and coherent optical manipulation for quantum information processing.

In regards to more complicated states, we explored the creation of a type of doubly excited super atom by applying a pulse sequence to create collective states, where the second pulse is detuned from the first to create a second excitation in the blockade volume. The excitation process is closely related to exciting Rydberg atom pair states. Double excitations create another spatial correlation between the atoms that depends on the Rydberg atom interaction potentials. Systems where this approach can most easily be investigated are lower energy Rydberg atom pair state potentials resulting from an avoided crossing. Regions of avoided crossings for Rydberg atom pairs are rather flat and can approximate a step-like potential allowing for a second excitation over a broad range of internuclear separations, R. The R at which these features naturally occur, or can be induced by the application of electric fields, are similar to useful blockade radii. At dipole trap densities, these

crossings also exist at R where there are more than 2 atoms that can be excited. Recall, blockade radii and curve crossings are common for $\sim 5\,\mu$m at $n \sim 60-90$, while the interatomic spacing at 10^{12} cm^{-3} is $\sim 1\,\mu$m. Lattices can also be superposed on the dipole trap within the cavity to further influence the spatial positions of the atoms relative to the cavity mode. Generally speaking, all these experiments are aimed at preparing Dicke and Dicke-like states in the cavity in a controlled way using Rydberg atom dipole blockade as a tool. Our research will help to advance our ability to engineer novel quantum states using Rydberg atom blockade and understand the excitation dynamics of super atoms and some higher order analogs.

Cavity Apparatus:

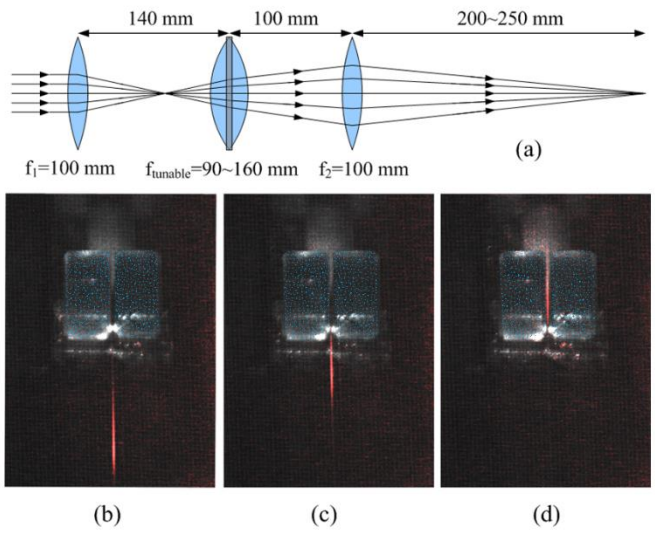

Figure 8: (a) Setup of the lens system for the dipole trap. The middle lens is a focus-tunable lens, which has a focal tuning range of 90 – 160mm, controlled by an applied current. (b-d) Fluorescence images that show the process of the atoms moving into the cavity.

The experimental system that was constructed consists of a Rb vapor cell MOT loaded, single beam, far-off resonance dipole trap (FORT) that is moved into a high finesse optical cavity with a voltage tunable lens (Optotune), Fig. 8. The transport distance is ~ 5 cm. Over this distance we observe no change in the size of the FORT, consistent with other work. The FORT distortion was verified with a CCD and knife edge tests. The FORT is created using a 25W Yb fiber laser at 1064 nm. The laser is focused to a ($1/e$) spot size of 50 μm for experiments. The temperature of the atoms in the FORT is $T = 40\mu$K. The FORT trap depth is around 1mK. Given the temperature and cavity mode volume, the fact that the trap relies on AC Stark shifts should not be a problem for the experiments, since the relevant coupling and decay rates exceed 1MHz for most of the experiments. A Rydberg atom blockade radius of 5 μm for a 10MHz bandwidth excitation is reasonable to achieve. Rydberg state selection and electric field tuning provide flexibility in changing the Rydberg blockade radius. At typical dipole trapping densities of 10^{12} cm^{-3} there are $\sim 10^4 - 10^5$ atoms in the mode volume of the cavity, depending on the dipole trap size used for the experiments. The number of atoms and density can be varied by changing the trap and loading parameters.

The apparatus we have constructed has several technical advantages over using single atom or N-atom trapping. The quantum state is ideally created in a dipole trap that can be used multiple times until background gas collisions deplete the trap. The approach eliminates the need to load fixed numbers of atoms into a dipole trap, cryogenics, bleaching of the source, blinking and difficult

fabrication techniques. The number of excitations inside the cavity is determined by the overlap of the state preparation region and mode volume of the cavity, the dipole blockade radius, and the sequence of laser pulses used to prepare the initial state.

We have developed all the necessary laser systems to carry-out Rydberg excitation experiments during this grant period. We use a home built doubling cavity to generate 480 nm and 780 nm light for Rydberg excitation in this experiment. We also have a 150mW 795 nm diode laser and a 35mW 476 nm diode laser that we have constructed for the cavity work. The 795 nm laser is locked to a Rb vapor cell while the 476 nm laser is locked to a home built Fabry-Perot cavity with an ultra-low expansion glass spacer held under vacuum. The spectral bandwidths of these laser systems are $\sim$500kHz or less, with the determination being limited by the fact that we have only tested them using EIT in a Rb vapor cell. The cooling and trapping lasers are completely independent.

The high finesse optical cavity is a standard tool in cavity quantum electrodynamics experiments. Typical, but not state-of-the-art, values of the atom cavity coupling constant, $g = 2\pi\times40$MHz, lengths, $\sim 100\ \mu$m, and mode volumes, $V = 2\times10^4\ \mu\text{m}^3$, are good enough for these experiments. The cavity that we built has $g \sim 2\pi \times 8.5$MHz with decay constants of $\kappa \sim 4$MHz and $\Gamma_0 = 6$MHz for Rb. The cavity length is $\sim 600\ \mu$m with a 150 μm gap so the atoms can be moved into the cavity and the preparation lasers can interact with the atoms. The radius of an achievable blockade volume, $R \sim 5\ \mu$m, is less than the dimensions of the optical cavity volume. Our calculations indicate that it is possible to reach a regime where the collectively excited atomic state spends enough time in the optical cavity to have a large probability to emit into the cavity mode and produce photons. We have other super polished mirrors to make different cavities including ones with both higher and lower finesse and larger and smaller cavity mode volumes.

Summary:

For this grant, we built an atom cavity apparatus to investigate single photon production using collective states created via Rydberg atom blockade. We studied the interaction between Rydberg atoms and surfaces because in the apparatus mirrors must be placed in close proximity to the atomic sample. We theoretically showed that different types of novel quantum states can be created in the cavity to produce quantum light. Seven papers were published in refereed journals describing this work. The work was presented in 22 different international conference venues, including 5 invited talks. In addition, the work was described in 10 different invited colloquia.

Papers:

1. "Exploiting Rydberg Atom Surface Phonon Polariton Coupling for Single Photon Subtraction," H. Kuebler, D. Booth, J. Sedlacek and J.P. Shaffer, Physical Review A **88**, 043810 (2013).

2. “Rydberg atom-based electric field sensing from radio to terahertz frequencies,” H.Q. Fan, S. Kumar, H. Kubler, S. Karimkashi and J.P. Shaffer, Journal of Physics B **48**, 202001 (2015) (invited Topical Review).

3. “Sub-wavelength microwave electric field imaging using Rydberg atoms inside atomic vapor cells,” H. Fan, S. Kumar, H. Kubler, R. Daschner and J.P. Shaffer, Optics Letters **39**, 3030 (2014).

4. “Interactions in Ultracold Rydberg Gases,” J. P. Shaffer and L.G. Marcassa, Advances in Atomic, Molecular and Optical Physics (invited), Advances in Atomic, Molecular and Optical Physics **63**, 47 (2014).

5. “Coherent collective state synthesis in an optical cavity using Rydberg atom dipole blockade,” S. Kumar, J. Sheng, J. Sedlacek, H.Q. Fan and J.P. Shaffer, Journal of Physics B (Special Issue on Rydberg Atom Physics) **49**, 064014 (2016).

6. “The role of multi-level Rydberg interaction in electric field tuned Forster resonances,” Jorge M. Kondo, D. Booth, Luís F. Gonçalves, J.P.Shaffer and Luis G. Marcassa, Physical Review A **93**, 012703 (2016).

7. “Neutralization of Surface Adsorbate Electric Fields of Rubidium by Slow Electron Attachment,” J.A. Sedelacek, E. Kim, S. T. Rittenhouse, P.F. Weck, H. Sadeghpour and J.P. Shaffer, Physical Review Letters **116**, 133201 (2016).

Conference Talks and Presentations:

1. “Anisotropic Rydberg Atom Interactions,” D. Booth, J. Tallant and J.P. Shaffer, DAMOP, Los Angeles, CA (2012).

2. “Polarization Dependent Dark Resonances in Electromagnetically Induced Transparency with Rydberg Atoms,” J. Sedlacek, A. Schwettmann, H. Fan and J.P. Shaffer, DAMOP, Los Angeles, CA (2012).

3. “Using Rydberg Atom Electromagnetically Induced Transparency for Microwave Electrometry Applications,” J. Sedlacek, H. Fan, R. Daschner, C. Ewel, H. Kubler and J.P. Shaffer, DAMOP, Quebec City, Quebec, Canada (2013).

4. “Progress Toward Coupling a Sample of Collectively Excited Atoms to a High Finesse Cavity,” P. Zabawa, C. Ewel, H. Kubler, and J.P. Shaffer, DAMOP, Quebec City, Quebec, Canada (2013).

5. "Sub-wavelength Microwave Electric Field Imaging using Rydberg Atoms," H.Q. Fan, S. Kumar, R. Daschner, H. Kubler, and J.P. Shaffer, DAMOP, Madison WI (2014).

6. "Coherent Manipulation by adiabatic passage of interacting Rydberg atoms inside a cavity," S. Kumar, C. Ewel, J. Sedlacek, J.P. Shaffer, DAMOP, Madison WI (2014).

7. "Probing Atom Surface Interactions Using Rb Rydberg Atoms," J. Sedlacek, H. Kubler, C. Ewel and J.P. Shaffer, DAMOP, Madison WI (2014).

8. “Using Rubidium Rydberg Atoms to Probe Atom-Surface Interactions,” J. Sedlacek and J.P Shaffer, 2nd International Conference on Rydberg Atom Physics, Recife, Brazil (2014).

9. "Coherent Control of Strongly Interacting Rydberg Gases in Thermal Vapor Cells," H. Kubler, R. Low, J.P. Shaffer and T. Pfau, 2nd International Conference on Rydberg Atom Physics, Recife, Brazil (2014). ***(invited)***

10. "Production of a 2-D Electron Gas Using Rydberg Atoms and Surface Adsorbates," J.P. Shaffer, B2 conference on Quantum Hybrid Systems, Tucson, AZ (2015). ***(invited)***

11. "Atom-surface Studies with Rb Rydberg Atoms," Y. Chao, J. Sheng, J. Sedlacek and J.P. Shaffer, DAMOP, Columbus, OH (2015).

12. "Homodyne Microwave Electric Field Measurements Using Cs Rydberg Atoms in Vapor Cells," H. Fan, S. Kumar and J.P. Shaffer, DAMOP, Columbus, OH (2015).

13. "Interacting Rydberg Atoms in an Optical Cavity to Synthesize Coherent Collective States using Dipole Blockade," J. Sheng, J. Sedlacek, C. Ewel, H. Fan and J.P. Shaffer, DAMOP, Columbus, OH (2015).

14. "Rydberg Blockaded Medium Inside a High-Finesse Optical Cavity," J. Sheng, S. Kumar, W. Whiteneck, J. Sedlacek and J.P. Shaffer, DAMOP, Columbus, OH (2015).

15. "The Role of 2-Body Interaction on the Broadening of a Forster Resonance," J. Kondo, L. Goncalves, J. Tallant, D. Booth, J.P. Shaffer and L.M. Marcassa, DAMOP, Columbus, OH (2015).

16. "Neutralization of Rb Surface Adsorbate Electric Fields by Slow Electron Attachment," J. Sedlacek, G. Chao and J.P. Shaffer, DAMOP, Columbus, OH (2015).

17. "Electric field cancellation on quartz by Rb adsorbate-induced negative electron affinity," J.P. Shaffer, DAMOP, Providence, RI (2016). (***invited)***

18. "The importance of multi-level Rydberg interaction in electric field tuned Forster resonances," J. Kondo, D. Booth, L. Goncalves, J.P. Shaffer and L. Marcassa, DAMOP, Providence, RI (2016).

19. "Electromagnetically induced transparency with Rydberg atoms inside a high-finesse optical cavity," J. Sheng, S. Kumar, J. Sedlacek, Y. Chao, H. Fan and J.P. Shaffer, DAMOP, Providence, RI (2016).

20. "Engineered Rydberg Atom-Surface Interactions Using Metamaterials," Y. Chao, J. Sheng, J. Sedlacek, and J.P. Shaffer, DAMOP, Providence, RI (2016).

21. "Electric field cancellation on quartz by Rb adsorbate-induced negative electron affinity," J.P. Shaffer, Correlation and Order in Rydberg Gases, Lorentz Center, Leiden, Netherlands (2016). (***invited)***

22. "Electric field cancellation on quartz by Rb adsorbate-induced negative electron affinity," J.P. Shaffer, LAOP, Medellin, Colombia (2016). (***invited)***

Invited Colloquia:

1. "Interactions and Novel Forms of Matter in Ultracold Rydberg Gases," J.P. Shaffer, University of Oklahoma (2012).

2. “Quantum Assisted Sensing Using Rydberg Atom Electromagnetically Induced Transparency,” J.P. Shaffer, State Key Laboratory of Magnetic Resonance and Atomic and Molecular Physics, Wuhan Institute of Physics and Mathematics, Chinese Academy of Sciences, Wuhan 430071, China (2013).

3. “Interactions and Novel Forms of Matter in Ultracold Rydberg Gases,” J.P. Shaffer, State Key Laboratory of Magnetic Resonance and Atomic and Molecular Physics, Wuhan Institute of Physics and Mathematics, Chinese Academy of Sciences, Wuhan 430071, China (2013).

4. “Interactions and Novel Forms of Matter in Ultracold Rydberg Gases,” J.P. Shaffer, Shanxi University, Tiyuan , China (2013).

5. “Interactions and Novel Forms of Matter in Ultracold Rydberg Gases,” J.P. Shaffer, Rice University (2013).

6. “Novel States of Ultracold Rydberg Atoms and Some of their Applications,” Texas A&M, Commerce (2015).

7. “Electric field cancellation on quartz by Rb Adsorbate-Induced Negative Electron Affinity,” University of Michigan, Ann Arbor (2016).

8. “Electric Field Cancellation on Quartz by Rb Adsorbate-Induced Negative Electron Affinity and Rydberg Atom Surface Interactions” University of Sao Paulo, Sao Carlos, Brazil (2016).

9. “Electric Field Cancellation on Quartz by Rb Adsorbate-Induced Negative Electron Affinity and Rydberg Atom Surface Interactions” University of Sao Paulo, Sao Paulo, Brazil (2016).

10. “Electric field cancellation on quartz by Rb adsorbate-induced negative electron affinity,” J.P. Shaffer, University of Stuttgart (2016).